DOI:10.5937/jaes0-35514
Paper number: 20(2022)3, 975, 688-699
*www.engineeringscience.rs * ISSN 1451-4117 * Vol. 20, No 3, 2022*

THE RESEARCH OF REINFORCED CEMENT LINER FOR RECONSTRUCTION OF WATER SUPPLY AND SEWER PIPES

Elena Makisha
Moscow State University of Civil Engineering, 26, Yaroslavskoye shosse, Moscow, Russia
**makishaev@mgsu.ru*

The research is focused on the investigation of the features of mortar liner reinforced with composite mesh, which may be one of the possible options in case of one possible method of trenchless reconstruction of water and sewer pipes. The research had two goals: to study the strength under static loading of a mortar liner reinforced with a composite mesh frame and to define the maximum depth of underground location of a coating element, which is of significant importance if a host pipe cannot bear external loads any longer. Within the research, two specimens of coating with the length of 1000 mm and diameter of 800 mm were tested. The compression results showed that for both specimens the loss of bearing capacity occurred to the fluidity of composite reinforcement under the load of approximately 30 kN. After the strength test, a calculation was made to evaluate the maximum depth of liner location in case if a host pipe fully exhausts its bearing capacity. The results of the calculation showed that the maximum height of the soil layer above the crown of a pipe is 2.8 to 3.2 m depending on the type and features of the soil.

Keywords: water suppl, sewer; pipe, reconstruction, mortar coating, cement liner, reinforcement, pipe strength, bearing capacity

1 INTRODUCTION

Reliability and environmental safety are the main requirements applied to modern wastewater disposal systems. In general, reliability may be considered as the feature of an object to perform specified functions and to maintain the values of operational parameters in time and within the specified limits corresponding to the specified modes and conditions of use [1]. Reliability in general unites and includes several single properties: durability, maintainability, operational controllability and safety, etc. [2].

A drainage system from the viewpoint of reliability can be considered either as an entire system or as a combination of its certain elements: pumping stations, sewage treatment plants, gravity networks, and pressure sewer pipelines [3]. Some water pipelines have been in service for decades, which may result in significant wear of pressure and gravity pipelines, can increase the risk of accidents, and therefore, strongly affect their reliability [4]. The selection reconstruction approach conventionally depends on the failure mechanism and host pipe condition, including the degree of corrosion, structural deterioration, and hydraulic capacity loss [5].

Compared with traditional open-cut methods, trenchless reconstruction of water and sewer pipes has certain advantages: cost-efficiency of being cost-effective, less disturbance to the ground (traffic and residents), less environmental impact, and fast construction [4, 6].

The main direction of the trenchless restoration of underground pipelines considers the application of internal protective coatings (linings, shells, jackets, membranes, inserts, etc.), which may cover the host pipe along the entire length or individual defects.

Among the variety of trenchless methods of water supply and drainage networks restoration, the following approaches can be pointed out:

spray in place (SIP) is the application of spraying coatings on the inner surface. One of the possible options is a cement mortar liner or a cement coating sprayed on the surface of the inner walls of the existing pipe [7,8];

cured in place pipe (CIPP) rehabilitation of the pipelines through a flexible (thermosetting) liner, which is inserted into an existing pipe [9];

sliplining is the method of pipe reconstruction when a new pipe is inserted into a deteriorated host pipe [10,11];

modified sliplining is a method of rehabilitation of host pipe with a spiral wound [12];

lining with inserted flexible polymeric hose [13].

Each of the listed methods of restoration has certain specific features, which determine the scope of their application to restore water supply and drainage networks. The choice and further implementation of a particular method require a detailed preliminary inspection to investigate the condition of the pipeline, its dimensions, the type of transported medium, the surrounding underground infrastructure, the type of soil, the presence of groundwater, etc. [14, 15].

Among the well-known methods of rehabilitation, cement spraying can be considered as one of the oldest with an experience of implementation since the early 1900s. The main advantages of cement liner are the coating strength and evident anticorrosion properties [16]. The use of mortar liner should be considered, first, as anti-corrosive insulation of the inner surface of pipelines. A special property of the cement-based coating provides passive and active effects. The passive effect is achieved due to the mechanical insulation of the pipe walls with a strong protective layer, and the active effect is based on the formation of a saturated solution of calcium hydroxide with pH = 12.6 on the interface of the cement coating and the pipe wall. Under these conditions, low-alloy steel does not corrode [17]. At the same time, the mortar coating has the property of self-treatment. It consists of the fact that cracks and crevices that may occur during the application and setting of the solution are self-sealed both due to the swelling of the material and the calcareous deposits released in the form of calcium carbonate [18].

While remaining in demand today, mortar liners are being gradually replaced with the new polymer of composite materials. One of the options for the improvement of mortar coatings is their reinforcement to increase strength characteristics. Application of reinforced coating may be especially reasoned if the partially deteriorated host pipeline turns to full deterioration and loses its strength [19, 20].

The research had two goals. The first was to study the strength under static loading of a coating element made of a cement-sand base and reinforced with a composite mesh frame. The obtained bearing capacity of a coating element may play a significant role if the host pipeline cannot provide load-bearing capacity (coating becomes an in-dependent pipeline), or maybe considered as additional strength of combined structure (host pipe+coating). The second goal was to define the maximum depth of under-ground location of a coating element, which is of significant importance if a host pipe cannot bear external loads any longer. Thus, both research goals complement each other.

2 MATERIALS AND METHODS

2.1 Specimen

There were two specimens (Figs.1 and 2) manufactured for the research to imitate the cylindrical segment of inner cement coating of a host pipeline. The mortar liner specimen was reinforced with mesh frame of composite fiber (fig. 3 a, b).

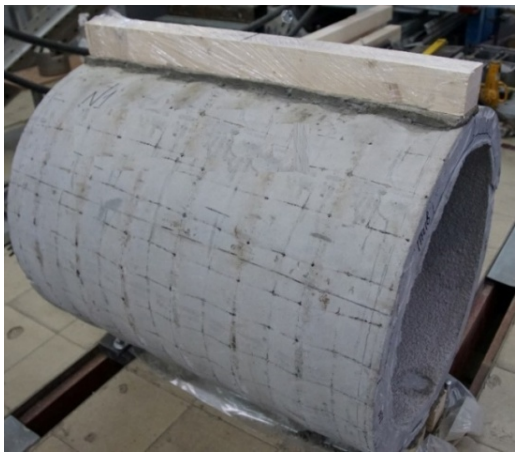

Figure 1. Photo of the specimen #1

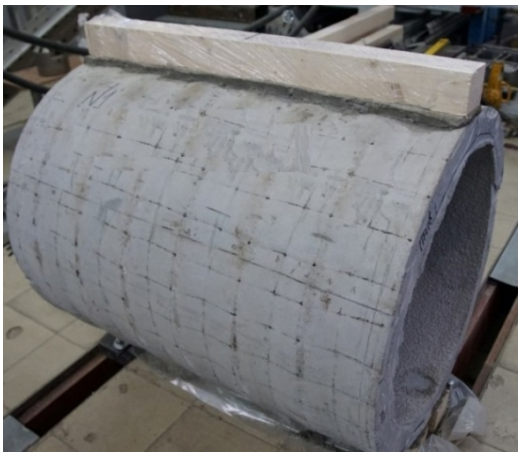

Figure 2. Photo of the specimen #2

a)

b)

Figure 3. Composite reinforcement: a – reinforcement mesh frame; b – specimen of reinforcement

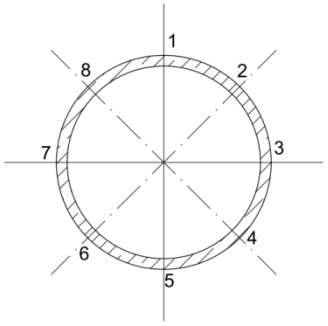

Figure 4. Location of control points for measuring the wall thickness

Both specimens had a length of 1000 mm and an outer diameter of 800 mm. Before the research commenced, wall thickness of each specimen were measured. Location of control points for measuring the wall thickness are shown in the fig. 4. Wall thickness of the specimens is presented in Table 1.

Table 1. Wall thickness measurements of concrete pipe specimens

Control points	Wall thickness [mm]	
	Specimen #1	Specimen #2
1	71.33	79.70
2	81.30	73.03
3	81.40	78.10
4	85.74	75.53
5	84.75	70.00
6	74.64	67.12
7	67.79	77.16
8	70.59	67.00
Mean value [mm]	77.19	73.46
Mean square deviation [mm]	6.95	4.96
Coefficient of variation [%]	9.00	6.76

2.2 Test sequence

The tests were carried out in accordance with the requirements of standard of Russian Federation “GOST 6482-2011 “Reinforced concrete non-pressure pipes. Specifications” (Fig.5) [21]. The experiment procedure was very similar to procedure in [22], which is typical for strength research, e.g. research of De La Fuente et al. [23] and Park et al [24].

The following sequence of experiment was applied:

A cylindrical specimen of reinforced cement coating was placed horizontally on two wooden beams laid parallel to the longitudinal axis of the pipe on a fixed base (the power floor of the laboratory). A wooden beam was laid along the crown of the pipe with a steel traverse installed on it. Dimensions (cross section) of a wooden beam was 80x80 mm.

A leveling layer of cement-sand mortar was laid under the upper and lower beams to provide even load to the specimens.

Loading of the specimen was carried out gradually with the step of 5 kN/m = 500 kg/m, using hydraulic jacks equipped with displacement and load sensors. The load increase was carried out evenly for 2-3 minutes, after which it was maintained for 10 minutes. The maximum possible load that was applied to the specimens was 33 kN/m.

The loading stage corresponding to the moment of cracking was determined by visual inspection (using a Brinell microscope). After the crack formation load, the crack formation was monitored and the crack opening value was measured with a measurement error of 0.01 mm).

Loading was applied until the bearing capacity of the specimen was exhausted, characterized by one of the following states:

fluidity of composite reinforcement, characterized by a crack opening width of more than 1.5 mm in pipes with a double frame and more than 2 mm in pipes with a single frame;

crushing of concrete from compression;

rupture of spiral fittings;

delamination of the pipe wall (separation of fittings in a pipe top or tray).

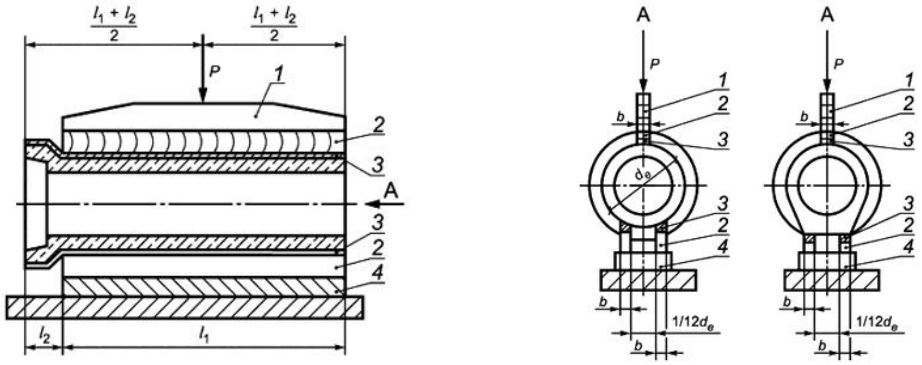

Figure 5. Loading scheme [21]: 1 – traverse; 2 - wooden beams; 3 – rubber gaskets or cement-sand mortar; 4 – basement.

3 RESULTS

Figures 6 shows the loading scheme of the specimen and the location of the linear displacement sensors, which were used to determine the deviation of the geometric dimensions relative to the initial state. The appearance of the specimens after the test is shown in figures 7 and 8.

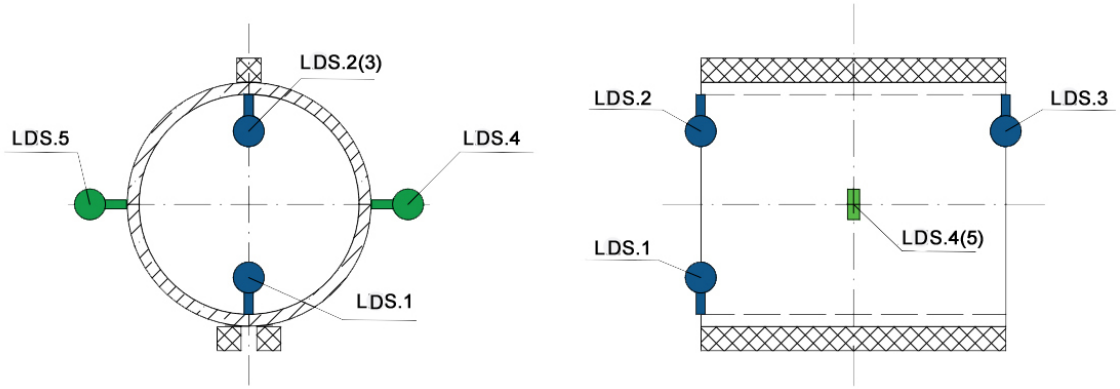

Figure 6. Location of linear displacement sensors (LDS): LDS.1, LDS.2, LDS.3 – sensors of linear vertical displacements of the specimen walls; LDS.4, LDS.5 – sensors of linear horizontal displacements of the specimen walls

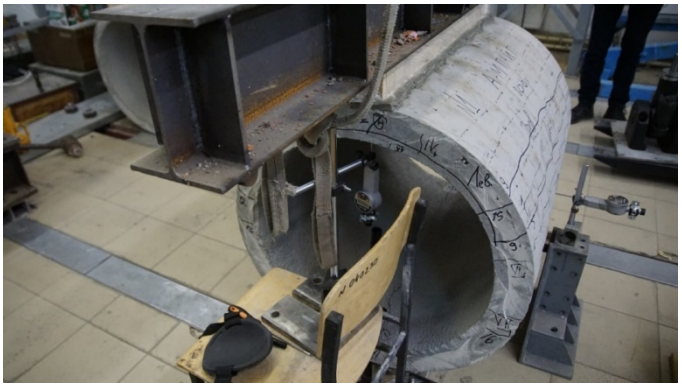

Figure 7. Specimen #1 after test

Figure 8. Crack of the width of 2mm inside the specimen#2

Tables 2 and 3 show the summary of the displacement based on data of sensors installed on specimens #1 and #2, respectively.

According to the testing method, the maximum load perceived by the specimen was estimated by the crack opening width. Tables 4 and 5 show data on the width of the cracks, which were formed because of the loading of specimen #1. As can be seen, for specimen #1, the load value at which the specimen lost its bearing capacity was 31 kN.

Table 2. Displacement measuring for specimen #1

Distributed load on the specimen [kN/m]	Indications of linear displacement sensors [mm]				
	LDS.1	LDS.2	LDS.3	LDS.4	LDS.5
`1	0.00	0.00	0.00	0.00	0.00
6	0.01	0.01	0.00	0.01	0.01
6*	0.01	0.01	0.00	0.01	0.01
11	0.09	0.17	-0.10	0.10	0.00
11*	0.09	0.17	-0.10	0.10	0.00
16	0.22	0.43	0.05	0.56	-0.37
16*	0.30	0.56	0.22	0.77	-0.50
21	0.23	2.98	2.53	2.18	0.83
21*	0.22	3.54	3.21	2.39	1.08
26	0.18	5.14	4.39	3.10	2.09
26*	0.17	5.82	4.96	3.25	2.33
31	0.02	7.31	6.55	3.79	3.29
31*	0.01	7.77	7.01	3.96	3.62

Table 3. Displacement measuring for specimen #2

Distributed load on the specimen [kN/m]	Indications of linear displacement sensors [mm]				
	LDS.1	LDS.2	LDS.3	LDS.4	LDS.5
1	0.00	0.00	0.00	0.00	0.00
3	-0.07	0.05	0.04	0.31	-0.03
3*	-0.08	0.10	-0.04	0.37	-0.35
6	-0.14	-0.15	0.14	0.54	-0.51
6*	-0.15	0.44	0.13	0.56	-0.53
9	-0.20	0.50	0.20	0.49	-0.43
9*	-0.20	0.52	0.22	0.49	-0.43
12	-0.24	0.57	0.29	0.39	-0.32
12*	-0.24	0.58	0.34	0.39	-0.29
15	-0.28	0.63	0.42	0.35	-0.22
15*	-0.28	0.57	0.47	0.34	-0.20
18	-0.33	0.74	0.64	0.40	-0.19
18*	-0.34	0.77	0.71	0.36	-0.10
21	-0.37	1.21	1.13	0.36	0.42
21*	-0.38	1.44	1.31	0.42	0.49
24	-0.39	2.08	1.99	0.63	0.94

Distributed load on the specimen [kN/m]	Indications of linear displacement sensors [mm]				
	LDS.1	LDS.2	LDS.3	LDS.4	LDS.5
24*	-0.39	2.34	2.37	0.75	1.05
27	-0.33	3.84	3.68	2.12	2.18
27*	-0.33	3.84	5.10	2.35	2.38
30	-0.34	4.13	5.62	2.64	2.65
30*	-0.36	4.51	6.31	2.83	2.65
33	-0.37	5.2	7.21	3.24	2.82
33*	-0.37	5.58	7.63	3.46	2.97

Table 4. Results of measurements of cracks on the lateral surface of the specimen #1

Crack number on the lateral surface	Distributed load on the specimen					
	21 kN/m	21* kN/m	26 kN/m	26* kN/m	31 kN/m	31* kN/m
I	0.05/1000	0.05/1000	0.20/1000	0.20/1000	0.30/1000	0.30/1000
II	0.10/1000	0.10/1000	0.25/1000	0.25/1000	0.30/1000	0.30/1000
III	0.05/1000	0.05/1000	0.15/1000	0.15/1000	0.25/1000	0.25/1000
IV	0.05/1000	0.05/1000	0.15/1000	0.15/1000	0.15/1000	0.15/1000
V	0.05/1000	0.05/1000	0.30/1000	0.30/1000	0.30/1000	0.30/1000
VI	0.20/1000	0.20/1000	0.35/1000	0.35/1000	0.40/1000	0.40/1000
VII			0.20/1000	0.20/1000	0.25/1000	0.25/1000
VIII			0.15/1000	0.15/1000	0.15/1000	0.15/1000
IX					0.15/1000	0.15/1000
X					0.30/165	0.30/165
XI					0.05/1000	0.05/1000
XII					0.10/1000	0.10/1000

Note:Here and in the tables 5-7:

1. The value of "X/Y" = "crack opening width “X” mm /crack length “Y” mm".

2. The value of the opening at a distributed load with the symbol "" is indicated after exposure under load for 10 minutes in accordance with the loading procedure.*

Table 5. Results of measurements of cracks on the end surface of the specimen #1

Crack number on the endsurface	Distributed load					
	21 kN/m	21* kN/m	26 kN/m	26* kN/m	31 kN/m	31* kN/m
I	0.50/35	0.50/35	1.00/58	1.00/58	1.30/58	1.30/58
II	0.80/55	0.80/55	1.20/55	1.20/55	1.30/60	1.30/60
III	1.00/22	1.00/22	1.20/22	1.20/22	1.50/22	1.50/22
IV	0.30/30	0.30/30	0.35/30	0.35/30	0.35/53	0.35/53
V	0.70/20	0.70/20	1.10/20	1.10/20	1.50/20	1.50/20
VI	0.30/67	0.30/67	0.20/67	0.20/67	0.40/67	0.40/67
VII	0.20/80	0.20/80	0.35/83	0.35/83	0.40/83	0.40/83
VIII	1.00/75	1.00/75	1.30/75	1.30/75	2.00/75	2.00/75
IX			0.15/67	0.15/67	0.30/67	0.30/67

Crack number on the endsurface	Distributed load					
	21 kN/m	21* kN/m	26 kN/m	26* kN/m	31 kN/m	31* kN/m
X			0.25/25	0.25/25	0.30/35	0.30/35
XI			0.15/65	0.15/65	0.25/65	0.25/65
XII			0.15/41	0.15/41		
XIII			0.15/27	0.15/27		
XIV			0.35/80	0.35/80	0.80/80	0.80/80
XV					0.05/65	0.05/65
XVI					0.15/60	0.15/60
XVII					0.15/23	0.15/23
XVIII					0.20/25	0.20/25
XIX					0.25/18	0.25/18
XX					0.15/35	0.15/35
XXI					0.15/50	0.15/50
XXII					0.10/24	0.10/24

Tables 6 and 7 show data on the width of the cracks, which were formed because of the loading of specimen #2. The maximum load was equal to 30 kN for specimen #2.

Table 6. Results of measurements of cracks on the lateral surface of the specimen #2

Crack number on the lateral surface	Distributed load					
	27 kN/m	27* kN/m	30 kN/m	30* kN/m	33 kN/m	33* kN/m
I	0.20/1000	0.20/1000	0.20/1000	0.20/1000	0.20/1000	0.20/1000
II	0.15/1000	0.15/1000	0.25/1000	0.25/1000	0.25/1000	0.25/1000
III	0.20/1000	0.20/1000	0.20/1000	0.20/1000	0.20/1000	0.20/1000
IV	0.15/430	0.15/430	0.20/430	0.20/430	0.2/460	0.2/460
V	0.20/1000	0.20/1000	0.20/1000	0.20/1000	0.20/1000	0.20/1000
VI	0.05/1000	0.05/1000	0.15/1000	0.15/1000	0.15/1000	0.15/1000
VII			0.10/1000	0.10/1000	0.20/1000	0.20/1000
VIII			0.15/1000	0.15/1000	0.15/1000	0.15/1000
IX			0.25/1000	0.25/1000	0.25/1000	0.25/1000
X			0.20/1000	0.20/1000	0.25/1000	0.25/1000
XI			0.10/1000	0.10/1000	0.10/1000	0.10/1000
XII			0.10/1000	0.10/1000	0.15/1000	0.15/1000

Table 7. Results of measurements of cracks on the end surface of the specimen #2

Crack number on the end surface	Distributed load								
	21 kN/m	21* kN/m	24 kN/m	24 * kN/m	27 kN/m	27* kN/m	30 kN/m	30* kN/m	33 kN/m
I	0.25/60	0.25/60	0.25/60	0.15/60	0.05/60	0.05/60	0.05/76	0.05/76	0.10/89
II	0.20/27	0.20/27	0.30/27	0.40/27	0.20/27	0.20/27	0.20/27	0.20/27	0.20/27
III	0.10/50	0.10/50	0.30/50	0.30/50	1.00/50	1.00/50	1.30/50	1.30/50	1.60/50
IV	0.20/57	0.30/57	0.40/57	0.50/57	1.00/57	1.00/57	1.00/57	1.00/57	1.50/57

Crack number on the end surface	Distributed load								
	21 kN/m	21* kN/m	24 kN/m	24 * kN/m	27 kN/m	27* kN/m	30 kN/m	30* kN/m	33 kN/m
V			0.20/65	0.30/65	1.20/77	1.20/77	1.20/77	1.20/77	1.50/78
I'*			0.05/170	0.05/170	0.05/170	0.05/170	0.05/170	0.05/170	0.05/170
VI					0.10/23	0.10/23	0.20/68	0.20/68	0.25/68
VII					0.10/48	0.10/48	0.10/45	0.10/45	0.20/45
VIII					0.10/34	0.10/34	0.10/33	0.10/33	0.15/45
IX					0.70/68	0.70/68	0.80/68	0.80/68	1.40/68
X					0.10/54	0.10/54	0.15/55	0.15/55	0.20/55
XI					0.05/47	0.05/47	0.10/46	0.10/46	0.15/46
XII					0.10/43	0.10/43	0.10/42	0.10/42	0.10/42
XIII					0.10/23	0.10/23	0.20/24	0.20/24	0.10/42
XIV					0.10/47	0.10/47	0.15/45	0.15/45	0.20/45
XV					0.05/27	0.05/27	0.05/27	0.05/27	0.10/27
XVI					0.10/25	0.10/25	0.10/46	0.10/46	0.15/50
XVII					0.10/35	0.10/35	0.10/38	0.10/38	0.20/38
XVIII							0.05/30	0.05/30	0.05/30
XIX							0.05/32	0.05/32	0.05/32

Note: I' is a crack located along the circumference of the pipe.*

Figures 9 and 10 summarize the dependencies of displacement related to applied load for specimens #1 and #2, respectively. For specimen #1 (Fig.9), the measured displacement did not exceed 0.5 mm until the load reached the value of 15 kN. The next step of loading (+5kN) resulted in significant (5-6 times) growth of displacement, which was measured by sensors placed on the crown of the coating element. This means that the compressive strength of the cement component of the coating has been reached, and in the absence of reinforcement, this would lead to a loss of the bearing capacity of the entire coating element. Increase of the load until 30 kN led to the fluidity of composite reinforcement resulted in the crack opening, and consequently in the loss of bearing capacity.

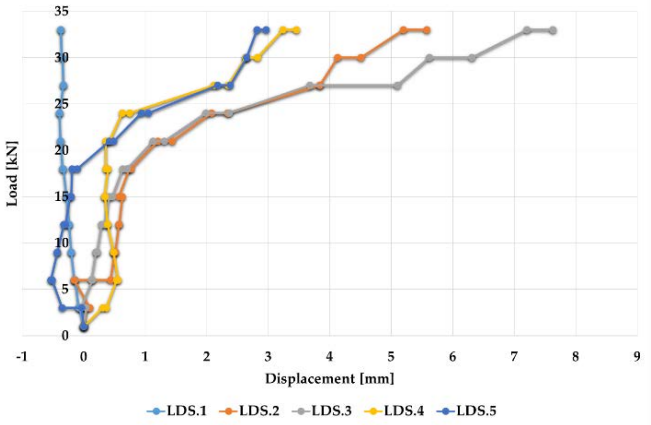

Figure 9. Diagram "Distributed load-displacement" for specimen #1

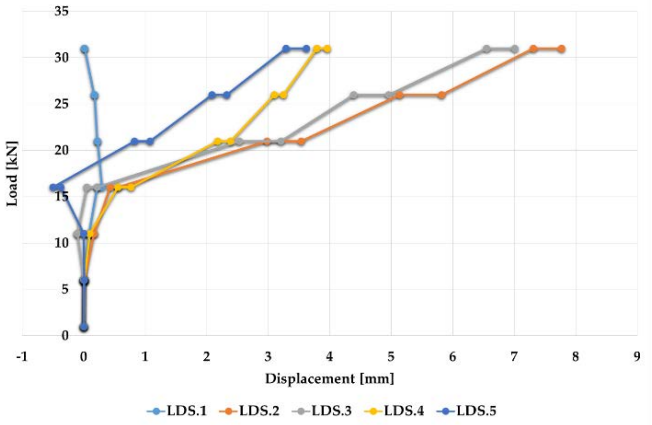

Figure 10. Diagram "Distributed load-displacement" for specimen #2

For specimen #2 (fig.10), the measured displacements did not exceed 0.5 mm until the load reached the value of 15 kN. The next step of loading (+5kN) showed only slight (double) growth of displacement. The further step of loading until 25 kN showed another double growth of displacement. Under the load of 33 kN, the loss of bearing capacity was reached due to the opening of cracks that meant the fluidity of composite reinforcement. For both specimens, displacements values measured under maximum loads were comparable. Obtained results correspond to existing practice, when a crack load and ultimate load relate to each other with a safety factor of 1.5 [25].

Following the test report, the permissible vertical load at which both tested specimens retained their bearing capacity (after being loaded for 10 minutes) was F = 30 kN.

The specimens' strength test is based on a standard for reinforced concrete pipes [21]. This document prescribes the division of pipes into 5 strength groups depending on their permissible depth: the maximum height of soil above the pipe crown is 2 m for group 1 and 10 m for group 5. Values of maximum height for groups 2, 3, and 4 are 4 m, 6 m, and 8 m, respectively.

For inner coatings (liners), which are applied for rehabilitation of partially deteriorated pipes; it is a matter of certain practical interest to estimate the maximum height of the soil layer above the crown of the pipe. If a host pipe fully deteriorates with the exhaustion of bearing capacity, the loads are perceived directly by the inner coating.

Based on the dependencies presented in [26] and [27], the permissible vertical pressure on the pipe (coating) can be estimated as follows:

$$P_{perm.} = \left(0.0186 + 0.025 \cdot \frac{y}{d_i}\right) \cdot \frac{F}{L \cdot y}, \quad (1)$$

where:

L is length of pipe (coating); L was equal to 1 m within this research;

y is the maximum vertical deformation (6.31 mm, see table 3);

d_i is the average inner diameter of the pipe/coating (see table 1 and 2):

for specimen #1 d_{i1} = 0.8 - 2·0.07719 = 0.64562 m;

for specimen #2 d_{i2} = 0.8 - 2·0.07346 = 0.65308 m.

The criterion for maintaining the bearing capacity of the pipe under the influence of vertical ground load can be determined with the inequality:

$$P_{perm.} \geq P_{\gamma}. \quad (2)$$

The normative vertical pressure of the soil P_y, may be determined using the equation [28]:

$$P_{\gamma} = C_{\gamma} \cdot \gamma_n \cdot h, \quad (3)$$

where:

h is the height of the soil layer above the crown of the pipe [m];

y_n is the normative specific weight of the soil [kN/m^3];

C_y is the vertical pressure coefficient, which is determined according to the following equation [28]:

$$C_{\gamma} = 1 + B \cdot \left(2 - B \cdot \frac{d}{h}\right) \cdot \tau_n \cdot \tan\varphi_n, \quad (4)$$

where:

d is the outer diameter of the coating element [m];

B is a width of the pipe foundation:

$$B = \frac{3}{\tau_n \cdot \tan\varphi_n} \cdot \frac{s \cdot a}{h}, \quad (5)$$

where:

φ_n is the normative angle of internal friction of the soil [27];

τ_n is the coefficient of the normative horizontal (lateral) pressure of the soil, determined by the formula [28]:

$$\tau_n = \tan^2\left(45^o - \varphi_n/2\right), \quad (6)$$

where:

a is the distance between the basement of the trench (undisturbed soil layer) and the crown of the coating element. For further calculation, *a* is assumed to be equal to 1 m (a sum of pipe foundation thickness (0.2 m) and outer diameter of the coating element (0.8 m));

s is the coefficient, which is equal to 1.0 when a pipe lays on soil foundation.

Based on the proposed sequence, a comparative calculation of the maximum height of the soil layer above the crown of the coating element for 4 different soils (sand, sandy loam, loam, clay) will be carried out. According to the reference data from [29], the following characteristics are accepted for calculation (Table 8). The calculation was made for the Dfb region according to Köppen climate classification [30].

Table 8. Characteristics of soils

Soil	Normative specific weight, y_n [kN/m^3]	Angle of internal friction, φ_n	
		min	max
Sand	16	26	43
Sandy loam	18	18	30
Loam	18,5	12	26
Clay	19,5	7	21

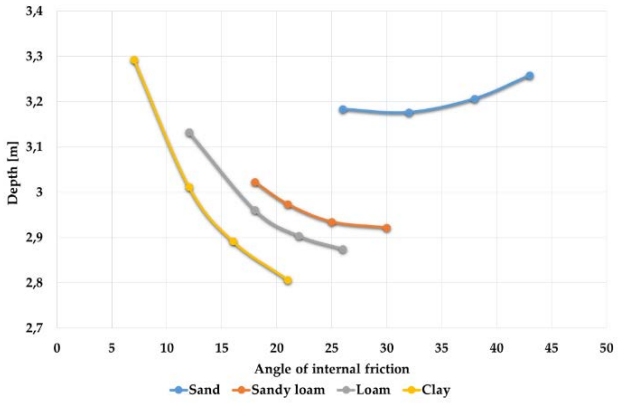

Figure 11. Determination of the height of the soil layer above the crown of the coating element

As it can be seen, in height of the sand soil layer is approximately 3.2 m regardless of the sub-type of the soil. On contrary, the sub-type of the clay soil may have a significant influence on conditions of coating application, with the soil height range between 2.8 and 3.3 m. For loam and sandy loam, the intermediate results are witnessed.

Thus, the investigated coating sample can be assigned to group 2 in terms of strength [21]. A review of standards for reinforced concrete pipes [26] provides the strength classes established for reinforced concrete pipes in various countries (China, New Zealand, Australia, Great Britain). The obtained value (30 kN) in all standards corresponds to the lowest strength class.

The review of literature sources showed that mechanical test of the stand-alone liner is not common; nevertheless, some results are available. Within their research, Roghanian and Banthia [31] studied non-reinforced cement coating and obtained approximately comparable results under a similar load test. However, in most cases, the object of the research is conventionally manufactured in factory reinforced concrete pipes directly [32, 33], or the joint work of the coating and the host pipe [7, 34, 35]. Within these researches, reinforced concrete pipes can normally withstand significantly higher loads than those obtained in our case, as far as the investigated coating element is not a pipe, but is sprayedinplace directly to the restored pipe, which may certainly affect its strength characteristics.

4 CONCLUSIONS

The performed research allowing making the following outputs:

- The research was aimed at a strength test of two specimens of sprayed-in-place cement (mortar liner) reinforced with composite fibers under the three-axis compression.
- The compression results showed that for both specimens the loss of bearing capacity occurred to the fluidity of composite reinforcement under the load of approximately 30 kN. The behavior of specimens under load corresponds to the common relation of crack load to ultimate load with the factor of 1.5.
- Obtained value of load approximately corresponds to the lowest class of reinforced concrete pipes according to the review of several standards.
- Analysis of obtained results showed that research of stand-alone liner without a host pipe is not common, however, available results may be considered as similar under comparable test conditions.
- After the strength test, a calculation was made to evaluate the maximum depth of liner location in case if a host pipe fully exhausts its bearing capacity. The results of the calculation showed that the maximum height of the soil layer above the crown of a pipe is 2.8 to 3.2 m depending on the type and features of the soil.

5 ACKNOWLEDGEMENT

This work was financially supported by the Ministry of Science and Higher Education (grant # 075-15-2021-686). All tests were carried out using research equipment of The Head Regional Shared Research Facilities of the Moscow State University of Civil Engineering

6 REFERENCES

[1] Zhou, X.; van Gelder, P.H.A.J.M.; Liang, Y.; Zhang, H. (2020). An integrated methodology for the supply reliability analysis of multi-product pipeline systems under pumps failure.Reliability Engineering & System Safety, vol. 204, 107185,DOI: 10.1016/j.ress.2020.107185

[2] Orlov, V.A. (2019). Ensuring physical integrity and energy saving in water transport pipeline systems after their reconstruction. Water and Ecology, Vol.24, no.4, 37-46, DOI:10.23968/2305-3488.2019.24.4.37-46

[3] Orlov, V.; Zotkin, S. (2018). Trenchless technology application of protective coatings that provide energy savings associated with transport of water via pipelines. Advances in Intelligent Systems and Computing, vol. 692,689-699, DOI:10.1007/978-3-319-70987-1_73

[4] Zhu, H.; Wang, T.; Wang, Y.; Li, V. C. (2021). Trenchless rehabilitation for concrete pipelines of water infrastructure: A review from the structural perspective.Cement and Concrete Composites, vol. 123,104193, DOI: 10.1016/j.cemconcomp.2021.104193

[5] Mohammadi, M. M.; Najafi, M.; Kaushal, V.; Serajiantehrani, R.; Salehabadi, N.; Ashoori, T. (2014). Sewer pipes condition prediction models: a state-of-the-art review.Infrastructure, vol. 4, 64, DOI: 10.3390/infrastructures4040064

[6] Orlov, V.; Andrianov, A. (2014). The selection of priority pipe sections for sewer network renovation", Applied Mechanics and Materials, vols.580-583,2398-2402, DOI:10.4028/www.scientific.net/AMM.580-583.2398

[7] Zhao, Y.; Ma, B.; Ariaratnam, S.T.; Zeng, C.; Yan, X.; Wang, F.; Wang, T.; Zhu, Z.; He, C.; Shi. G.; Mi, R. (2021). Structural performance of damaged rigid pipe rehabilitated by centrifugal spray on mortar liner. Tunnelling and Underground Space Technology, vol.116, 104117, DOI: 10.1016/j.tust.2021.104117

[8] Azoor, R.; Shannon, B.; Fu, G.; Deo, R.; Kodikara, J. (2021). Performance of field-aged polymeric spray lining for water pipe rehabilitation. Tunnelling and Underground Space Technology, vol.116, 104116. DOI: 10.1016/j.tust.2021.104116

[9] Das, S.; Bayat, A.; Gay, L.; Salimi, M.; Matthews, J. (2016). A comprehensive review on the challenges of cured-in-place pipe (CIPP) installations.Journal Of Water Supply: Research And Technology-Aqua, vol. 65,583–596, DOI: 10.2166/aqua.2016.119

[10] Rahmaninezhad, S. M.; Han, J.; Al-Naddaf, M.; Jawad, S.; Parsons, R. L.; Liu, H. (2020). Field evaluation of performance of corroded corrugated steel pipe before and after sliplining rehabilitation.Tunnelling and Underground Space Technology, vol.102, 103442, 2020 DOI: 10.1016/j.tust.2020.103442

[11] Wróbel, G.; Szymiczek, M.; Wierzbicki, Ł. (2004). Swagelining as a method of pipelines rehabilitation.Journal of Materials Processing Technology,vols. 157–158, 637-642, DOI: 10.1016/j.jmatprotec.2004.07.150

[12] Aşchileana, I.; Badea. G.; Giurca, I.; Naghiu, G.S.; Iloaie, F.G. (2017). Choosing the Optimal Technology to Rehabilitate the Pipes in Water Distribution Systems Using the AHP Method. Energy Procedia, vol.112, 19-26, DOI: 10.1016/j.egypro.2017.03.1109

[13] Lu, H.; Wu, X.; Ni, H.; Azimi, M.; Yan, X.; Niu, Y. (2020). Stress analysis of urban gas pipeline repairedby inserted hose lining method.Composites Part B: Engineering, vol.183, 107657, DOI: 10.1016/j.compositesb.2019.107657

[14] Scholten, L.; Scheidegger, A.; Reichert, P.; Mauer, M.; Lienert, J. (2014). Strategic rehabilitation planning of piped water networks using multi-criteria decision analysis. Water Resources,vol. 49,124-143, DOI: 10.1016/j.watres.2013.11.017

[15] Marlow, D.; Gould, S.; Lane, B. (2015). An expert system for assessing the technical and economic risk of pipe rehabilitation options.Expert Systems with Applications, vol. 42,8658-8668, DOI: 10.1016/j.eswa.2015.07.020

[16] Valix, M.; Zamri, D.; Mineyama, H.; Cheung, W. H.; Shi, J.; Bustamante, H. (2012). Microbiologically Induced Corrosion of Concrete and Protective Coatings in Gravity Sewers. Chinese Journal of Chemical Engineering,vol. 20,433-438, DOI:10.1016/S1004-9541(11)60150-X

[17] Grengg, C.; Mittermayr, F.; Ukrainczyk, N.; Koraimann, G.; Kienesberger, S.; Dietzel, M. (2018). Advances in concrete materials for sewer systems affected by microbial induced concrete corrosion: A review. Water Resources, vol. 134, 341-352, DOI: 10.1016/j.watres.2018.01.043

[18] Roychand, R.; Li, J.; De Silva, S.; Saberian, M.; Law. D.; Pramanik, B.K. (2021). Development of zero cement composite for the protection of concrete sewage pipes from corrosion and fatbergs. Resources, Conservation, Recycling,vol. 164, 105166, DOI: 10.1016/j.resconrec.2020.105166

[19] Scheperboer, I.C.; Luimes, R.A.; Suiker, A.S.J.; Bosco, E.; Clemens, F.H.L.R. (2021). Experimental-numerical study on the structural failure of concrete sewer pipes. Tunnelling and Underground Space Technology, vol.116, 104075, DOI: 10.1016/j.tust.2021.104075

[20] Mostafazadeh, M.; Abolmaali A. (2016). Shear behavior of synthetic fiber reinforced concrete.Advances in Civil Engineering Materials, vol, 5, no.1, 371-386, 2016DOI: 10.1520/ACEM20160005

[21] Standard of Russian Federation “GOST 6482-2011. Reinforced concrete non-pressure pipes. Specifications”. Available online: https://docs.cntd.ru/document/1200093396(access date: 14/11/2021)

[22] BSI BS EN 1916-2002 Concrete pipes and fittings, unreinforced, steel fibre and reinforced

[23] De la Fuente, A.; Escariz, R. C.; D.de Figueiredo, A.; Molins, C.; Aguado, A. (2012). A new design method for steel fibre reinforced concrete pipes. Construction And Building Materials, vol. 30, 547-555, DOI: 10.1016/j.conbuildmat.2011.12.015

[24] Park, Y.; Abolmaali, A.; Mohammadagha, M.; Lee, S. (2015). Structural performance of dry-cast rubberized concrete pipes with steel and synthetic fibers. Construction And Building Materials, vol. 77, 218-226, DOI: 10.1016/j.conbuildmat.2014.12.061

[25] Wong, L.S.; Nehdi, M.L. (2018). Critical Analysis of International Precast Concrete Pipe Standards. Infrastructures, vol.3, 18, DOI: 10.3390/infrastructures3030018

[26] Standard of Russian Federation “GOST R 54475-2011 Plastics structured-wall pipes and their fittings for sewerage systems outside the buildings. Specifications”https://docs.cntd.ru/document/1200087662 (access date: 14/11/2021)

[27] ISO 7685:1998. Plastics piping systems - Glass-reinforced thermosetting plastics (GRP) pipes - Determination of initial specific ring stiffness. Available online:https://docs.cntd.ru/document/1200102954 (access date: 14/11/2021)

[28] Construction code of Russian Federation “SP 35.13330.2011. Bridges and culverts”. Available online:https://docs.cntd.ru/document/1200084849 (access date: 14/11/2021)

[29] Construction code of Russian Federation “SP 22.13330.2016. Soil bases of buildings and structures”. Available online:https://docs.cntd.ru/document/456054206(access date: 14/11/2021)

[30] Kottek, M.; Grieser, J.; Beck, C.; Rudolf, B.; Rubel, F. (2006). World Map of the Köppen-Geiger climate classification updated”,Meteorologische Zeitschrift, vol. 15,259-263, DOI:10.1127/0941-2948/2006/0130.

[31] Roghanian, N.; Banthia, N. (2019). Development of a sustainable coating and repair material to prevent bio-corrosion in concrete sewer and wastewater pipes. Cement and Concrete Composites, vol. 100, 99-107, DOI:10.1016/j.cemconcomp.2019.03.026

[32] Kuliczkowska, E.; Kuliczkowski, A.; Tchórzewska-Cieślak, B. (2020). The structural integrity of water pipelines by considering the different loads. Engineering Failure Analysis, vol. 118, 104932, DOI: 10.1016/j.engfailanal.2020.104932

[33] Younis, A.-A.; Ramadan, A. S.; Wong, L. S.; Nehdi, M.L. (2020). New rational test for reinforced-concrete pipe eliminating subjective crack-width criteria. Structures, vol. 28,2507-2522, DOI: 10.1016/j.istruc.2020.10.076

[34] Zhang, X.; Fang, H.; Hu, Q.; Ma, B.; Hu, S.; Du, M.; Du, X.; Yang, K.; Li, B.; Shi, M. (2020). Mechanical performance of corroded reinforced concrete pipelines rehabilitated with sprayed-on cementitious liners subjected to combined loads.Tunnelling and Underground Space Technology, vol.103, 104266, DOI: 10.1016/j.tust.2021.104266

[35] Yang, K.; Fang, H.;Bu, J.; Zhang, X.; Li, B.; Du, X.; Zhang, Z. (2021). Full-scale experimental investigation of the mechanical characteristics of corroded buried concrete pipes after cured-in-place-pipe rehabilitation.Tunnelling and Underground Space Technology, vol.117, 104153, DOI: 10.1016/j.tust.2021.104153

Paper submitted: 22.12.2021.

Paper accepted: 13.01.2022.